Proceedings of IPC2002
4th International Pipeline Conference
September 29 – October 3, 2002, Calgary, Alberta, Canada

IPC02-27372

STRESS ANALYSIS OF PIPELINES WITH COMPOSITE REPAIRS

Luiz C.M. Meniconi
Petrobras Research Center (CENPES)

José L.F. Freire, Ronaldo D. Vieira, Jorge L.C. Diniz
Catholic University of Rio de Janeiro

ABSTRACT

The repair of corroded pipelines with fiber reinforced composite materials is a well-developed practice in the oil and gas transportation industry. Laboratory hydrostatic burst tests and field practice of several years have shown that these repairs are effective for pipelines with external corrosion defects. This paper deals with laboratory tests carried out to compare the behavior of fiber reinforced composite repairs applied to defects machined in pipeline test specimens.

The experimental results were compared to results from Finite Element Analysis (FEA) of the tubes tested. The parameters of FEA were calibrated to this specific problem, beforehand. Some hipotheses were tested during FEA trials to better explain the experimental results. The results indicated that, up to the starting of yielding of the pipe defected region, practically only the elastic pipe stresses equilibrate the pressure loading, due to the steel high Young modulus. After yielding, the composite material starts to work, carrying an important part of the pressure loading increments.

Experimental results also showed that the repair systems tested allowed the pipes to achieve the original design pressure before bursting. However, only one of the repair systems was approved in all strength verification tests for both internal and external defects. This system operated for four hours under a hydrostatic pressure test associated to the specified minimum yield strength (SMYS) of the steel and was also able to support ten pressure cycles of the design pressure afterwards, without showing any visual damage.

Keywords: composite sleeves, pipeline repairs, finite element analysis, hydrostatic tests.

INTRODUCTION

A research project was conducted to assess the behavior of composite repair systems from four different suppliers. Tubular specimens were provided with long artificial defects, simulating wall thickness reduction due to localized corrosion. The defects were made severe on purpose, with 70 percent loss of thickness, in order to investigate how far composite repair systems can reach. Severe as they were, the defects could still be repaired, according to ASME B31.4 code [1]. The reduction in internal pressure capacity of the tubes caused that type of defect is well known from previous studies [2].

After the specimens were repaired in the field, they were taken to the laboratory and a sequence of hydrostatic tests was performed to verify the ability of the repair systems to restore the original strength of the tubes.

EXPERIMENTAL PROCEDURES

Nine 20" nominal OD pipeline specimens of API 5L X60 steel were hydro tested. The specimens had machined internal or external defects, 500 mm long and 95 mm wide. Two tubes were not repaired. These specimens were tested up to rupture to demonstrate the loss of strength caused by the defects.

Figure 1 displays the geometry of the external defect introduced to the tubular specimen without composite reinforcement. The resulting thickness reductions for every specimen were carefully mapped. Further, steel samples were taken from every tube for tensile testing.

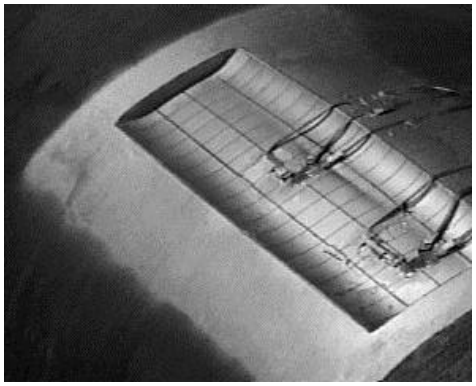

Figure 1 – External defect of a specimen without composite reinforcement, also showing the strain gage rosettes.

The OD of the tubes was 527 mm (20” nominal), they had a nominal thickness of 14.3 mm (0.562”) and were 3 meters long, with welded plane ends. The defects were milled till a depth to thickness ratio equal to 0.70 (10 mm depth). The borders of the milled region had a 50 mm fillet radius along the circumferential direction and a 12 mm fillet radius along the longitudinal direction. Figure 2 shows the field installation of a repair system.

Figure 2 – Field application of a composite repair.

Post yield strain gage rosettes were bonded to the steel surface of the pipes, two at region of the defect and another one halfway trough the end caps, to provide nominal strain figures.

Four commercial reinforcement systems were applied in the field. Seven specimens were repaired using systems named A, B, C and D. Systems A to C were applied to pipes that had machined internal or external longitudinal defects. The other system (D) was applied to a pipe with external defect.

The specimens were put inside a ditch up hill, parallel to an actual pipeline way. The experimental procedure aimed to simulate the real operation, where the repairs have to be applied in field conditions, which affect the quality of the resulting composite sleeves.

The field application also had the purpose of verifying the logistics of every repair supplier for the operation. This included the packing and preparation of materials, the necessary ancillary equipment and the number of personnel involved. The resulting installation time for a single repair was annotated. Attention was also given for the neatness of the whole process and the degree of site cleanness after the repair is done.

General details of the reinforcement systems and application procedures are given in Table1. The reinforcements were applied to the specimens containing water under a pressure of 5.05 MPa (51 bar). This pressure is the maximum pressure an actual pipe could operate containing a long defect with a maximum depth of 70 percent of the original wall thickness [1,3].

Table 1 - Details of the reinforcement systems.

Repair Properties	**Repair System**			
	A	B	C	D
Type of repair	Dry fiber glass fabric to be wrapped with impregnation of liquid resin	Ready pre-cured 1/8”layers ready to wrap around the pipe.	Flexible resin pre-impregnated bandage to be wrapped with water.	Flexible resin pre-impregnated bandage to be wrapped with water.
Application Procedure	1- Clean surface to white metal. 2- Apply filler to corrosion defect. 3- Apply resin to promote adherence between steel and composite.			
	4- Two different types of fiber-glass fabrics are wrapped around the pipe. Liquid resin is force-brushed between layers.	4- Wrap ready layers around the pipe using adhesive between wraps. 5- Apply external pressure to warrant tightness between layers.	4- Wrap ready flexible resin impregnated fabric around the pipe. Use water to help shape-curing the resin and promote adhesion between layers.	4- Wrap ready flexible resin impregnated fabric around the pipe. Use water to help shape-curing the resin and promote adhesion between layers.
Repair thickness	~ 25 mm	~ 25 mm	~ 25 mm	~ 25 mm
Application time	4 hours	1 hour	1 hour	1 hour
Curing time	24 hours	12 hours	12 hours	12 hours
E_1 [GPa]	18	27	28	8
E_2 [GPa]	10	12	12	6
S_{u1} [MPa] - ε_{u1} %	306 - 1.9	311 - 1.0	340 - 1.2	110 - 1.7
S_{u2} [MPa] - ε_{u2} %	99 - 1.4	21 - 0.2	150 - 2.0	75 - 1.5

After completion and cure of the composite repairs the tubes had their inside pressure alleviated and were transported to the lab to be submitted to hydrostatic test. Three other rosettes were bonded to the pipe specimens, on the composite surfaces. Two of them were installed over the defect region and care was taken so that they were in the same radial direction of the rosettes bonded to the steel defect surface. A third rosette was placed at a position 90° apart from the defect center. Figure 3 shows the general disposition of the sensors.

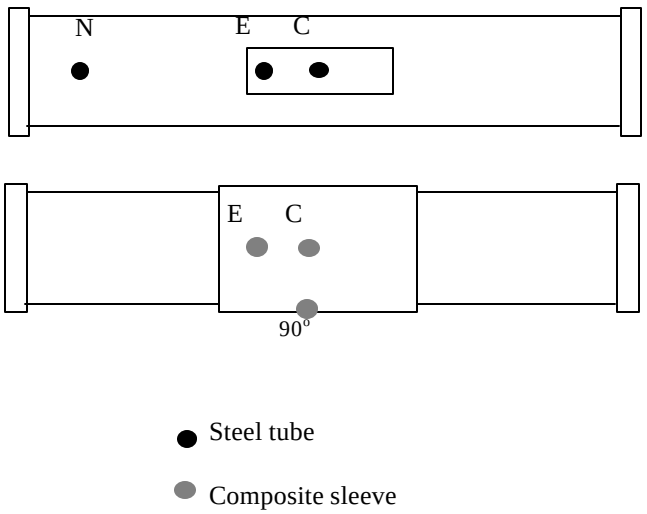

Figure 3 – Strain gage rosettes locations on the tubular specimens, both at metallic and composite surfaces.

The pressurizing system pumped de-aired water at a rate of 0.5 MPa/min (5 bar/min). The complete test procedure was composed of three pressure test cycles. The first test cycle pressurized the pipe specimens up to 90 percent of the design pressure of the pipeline. The specimens were unloaded and inspected to check for small leaks or reinforcement debonds. The rosettes were re-zeroed because some of them already indicated plastic strains (rosettes located inside the defect region).

The design pressure considers the SMYS of the pipe material decreased by a factor F=0.72 [1]. The design pressure is 16.8 MPa (171 bar). The second test cycle reached the design pressure and after that pumping continued until the pressure related to SMYS was reached. If the specimen were able to withstand this pressure for 4 hours, the pressure would be released to zero so that external inspection of the specimen and re-zeroing of the plastically deformed gages could be made. The third test cycle was composed of ten pressure cycles to the design pressure. Table 2 shows the test results.

Table 2 – Hydrotests results for the reinforced tubes.

2a – Internal defects.

Specimen	A	B	C
Depth/thickness d / t	0.68	0.68	0.67
S_u pipe[1] [MPa]	604	563	583
Burst pressure [MPa]	>23.4	20.2	23.4
Corrected non-repaired burst pressure[2] [MPa]	14.4	13.0	14.0
Strength ratio – corroded pipe[3]	>1.63	1.55	1.67
Strength ratio – non corroded pipe design pressure[4]	>1.39	1.20	1.39
Notes on test results	Passed all tests	Failed the SMYS test	Failed in time during SMYS test

2b – External defects.

Specimen	A	B	C	D
Depth/thickness d/t	0.69	0.70	0.66	0.72
S_u pipe[1] [MPa]	608	563	605	621
Burst pressure [MPa]	>23.4	19.2	>23.4	15.9
Corrected non-repaired burst pressure[2] [MPa]	13.9	12.4	15.0	13.0
Strength ratio – corroded pipe[3]	>1.68	1.55	>1.56	1.26
Strength ratio – non corroded pipe design pressure[4]	>1.39	1.14	>1.39	0.95
Notes on test results	Passed all tests	Failed the SMYS test	Passed all tests	Failed the design pressure test

OBS:

1 - Average ultimate strength of pipe material using 2 standard tension specimens.

2 - Corrected burst pressure calculated using DNV-RP101 [4], considering the average actual ultimate strength (see OBS 1) and actual defect d/t ratio.

3 - Actual burst pressure divided by the calculated burst pressure of the non-repaired pipe using actual material and d/t ratio; (see OBS 2).

4 - Actual burst pressure divided by the code [1] design pressure, calculated using nominal geometry and material properties.

The results related to the non-reinforced specimens were used as references or normalizing factors for comparison with the results of the reinforced specimens, as shown in table 2. The burst pressures were 14.6 MPa (149 bar) and 15.8 MPa (161 bar), for the non-reinforced tubes with external and internal defects, respectively. These pressures were approximately 90 percent of the original design pressure of the pipeline. The burst pressures predicted by DNV-RP101 [4] expression for rupture of single defects. were 14.0 MPa (143 bar) for the non-reinforced tube with external defect (the actual figure showed a difference of 4%) and 16.9 MPa (172 bar) for that with internal defect (a difference of -7%). The comparison was quite good.

As can be seen in Table 2 only one reinforcement system (A) passed all test cycles, considering both internal and external defects. System C supported the complete test cycle for the external defect specimen but the specimen with the internal defect failed the full hydrostatic pressure test after 30 minutes of maximum applied pressure. In general, failure was characterized by plastic collapse and leakage at the thinner section of the defect in the steel tube. The composite sleeves did not break. System B reached and passed the design pressures but failed before reaching the maximum hydrostatic test pressure for both specimens. System D failed near the design pressure. All systems presented reinforcement effects when compared to the burst pressures of the non-reinforced specimens. Systems A, B and C showed to withstand the design pressure with ratios of 1.39, 1.14 and 1.39.

FEA PROCEDURES

A preliminary task was to calibrate of the FEA parameters (element type and mesh size) to reproduce with sufficient accuracy an exact solution available in the literature for thick composite tubes. The validity of the "smearing" approach was checked. This considers the assembly of several alternate laminae to correspond to an equivalent specially orthotropic material. The objective was to define the simplest model that could still reproduce all the relevant characteristics of a thick composite tube.

An exact 3D solution was taken from Varadan and Bhaskar [5] for calibration purposes. They studied several configurations of layered tubes. A case was selected of a ($90^o/0^o/90^o$) layered laminated tube. Each layer had the same thickness in their case. The loading was an internal pressure q_i of the form:

$$q_i = -Q_0 \sin\left(\frac{mp\ z}{L}\right)\cos(nq)$$

where Q_0 is a constant positive pressure (resulting in a negative radial stress), z is the axial co-ordinate, L is the length of the tube and θ is the angular co-ordinate. The integers m and n were equal to 1 and 4, respectively. All the layers were made of the same material and the lamina properties were:

$$\frac{E_L}{E_T} = 25, \frac{G_{LT}}{E_T} = 0.5, \frac{G_{TT}}{E_T} = 0.2 \quad and \quad n_{LT} = n_{TT} = 0.25$$

where the subscript L refers to the longitudinal direction and the subscript T refers to the transverse direction. E are the Young's moduli, G are the shear moduli and ν are the Poisson's ratios. The results were given in terms of the following non-dimensional stresses:

$$\bar{s}_r = s_r \Big/ \left(Q_o \sin\left(\frac{mp\ z}{L}\right)\cos(nq)\right)$$

$$(\bar{s}_q, \bar{s}_z) = \left(\frac{10}{Q_0 S^2}\right)(s_q, s_z) \Big/ \left(\sin\left(\frac{mp\ z}{L}\right)\cos(nq)\right)$$

where r defines the radial direction of the tube and S is the average radius to thickness ratio, which was taken equal to 4.

Brick elements with 20 nodes were adopted, in a very fine mesh. There were 6 elements across the thickness. The FEA code used was ABAQUS [6]. The results are shown in fig. 4.

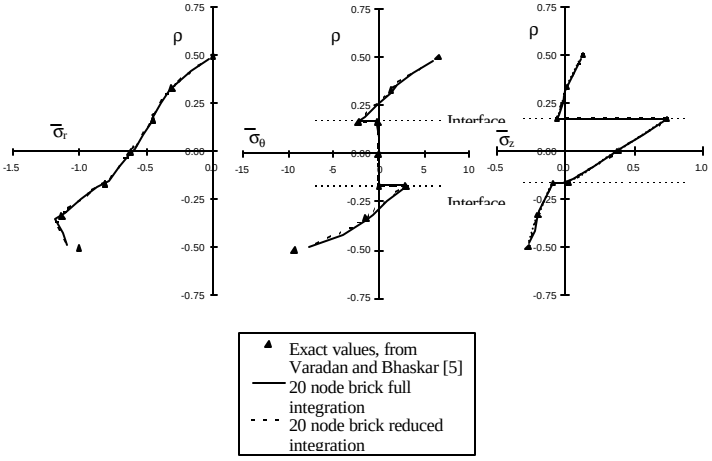

Figure 4 - Comparison between FEA and exact values, for a thick ($90^o/0^o/90^o$) layered laminated tube.

At first, a full integration brick element, with 27 Gaussian points was adopted. Later a more economical reduced integration scheme, with 8 Gaussian points was tried The parameter ρ is a non-dimensional radial co-ordinate, ranging from -0.5 at the inner surface to 0.5 at the outer one. The FEA results were taken at the integration points.

As can be seen, the agreement was very good, both for the full and the reduced integration elements. This result supported proceeding to the analysis of the composite tube reinforcements with the same sort of mesh parameters.

Once the basic FEA parameters have been defined, it is necessary to address the properties of the composite material to de adopted in the FEA model. Usually, the commercial repair systems constitute specially orthotropic materials, in which the important directions of the laminate coincide with the directions defined by the tube. In this case, 9 mechanical properties of the

material are in principle required, but this number is reduced due to the considerations that follow.

To simplify the discussion, take a unidirectional laminated material, where all fibers are disposed at the same direction. Normally, mechanical tests provide 4 basic properties of a lamina: the longitudinal modulus of elasticity, E_L or E_1, the transverse modulus of elasticity, E_T or E_2, the Poisson´s ratio in the plane of the lamina, ν_{LT} or ν_{12} and the shear modulus in the plane of the lamina of elasticity, G_{LT} or G_{12}.

A polar coordinate system was adopted for the FEA. The direction of the fibers (direction 1), that is the strongest within the laminated material, is made coincident with the circumferential direction (direction θ) of the tube, to better resist the hoop stress. The transverse direction of the lamina (direction 2) coincides with axial direction z of the tube. Direction 3, normal to the lamination plane, coincides with the radial direction r of the tube.

The nine required mechanical properties are E_1, E_2, E_3, G_{12}, G_{13}, G_{23}, ν_{12}, ν_{13} and ν_{23}. The out-of-plane properties are seldom measured, and it is usual to consider the material as isotropic in the transverse 2-3 plane. Some simplifications are:

$$E_2 = E_3 \quad , \quad G_{12} = G_{13} \quad and \quad \nu_{12} = \nu_{13}$$

In 2-3 plane the following relation is now valid:

$$G_{23} = \frac{E_2}{2(1+\nu_{23})}$$

The necessary properties are reduced to five. Four of them in the plane of the laminate, and thus easier to measure, as mentioned above: E_1, E_2, G_{12} and ν_{12}. The fifth required property, G_{23} (or ν_{23}, through the relation just shown) is obtained from the literature [7], as it is any other missing property.

Reciprocity relations lead to an useful expression, when it is necessary to convert from the lamina reference system to that of the tube:

$$\frac{\nu_{ij}}{E_i} = \frac{\nu_{ji}}{E_j}$$

Because it is made of an isotropic material, the steel tube requires only two properties: E and ν. As the experiments showed that the region within the machined defects went into plastic regime, the FEA models considered the stress versus strain curves measured for every metallic tube. To better account for the bulging effect, the FEA model also considered the geometric non-linearities that arise as the tube deforms under pressure.

The basic properties of the repair systems tested are given in table 1. Table 3 shows the values adopted for the remaining ones, obtained as discussed above.

Table 3 – Values adopted in the FEA models for the mechanical properties of the repair systems.

Elasticity modulus E_3	= E_2
Poisson´s ratio ν_{12}	0,3
Poisson´s ratio ν_{13}	= ν_{12}
Poisson´s ratio ν_{23}	0,4
Shear modulus G_{12}	4.0 GPa for unidirectional systems
Shear modulus G_{12}	7.0 GPa for clothe reinforcements
Shear modulus G_{13}	= G_{12}
Shear modulus G_{23}	= E_2 / 2 (1+ ν_{23})

The conversion to the polar reference system used in the FEA model of the tube from the laminated material reference system obeyed the convention shown in table 4.

Table 4 – Conversion to FEA reference system from lamina system.

FEA REF. SYSTEM	**LAMINA REF. SYSTEM**
Radial direction, 1.	Out-of-plane direction, 3.
Circumferential direction, 2.	Longitudinal direction, 1.
Axial direction, 3.	Transverse direction, 2.
E_1	E_3
E_2	E_1
E_3	E_2
ν_{12}	$\nu_{31} = (E_3/E_1) . \nu_{13}$
ν_{13}	$\nu_{32} = (E_3/E_2) . \nu_{23} = \nu_{23}$
ν_{23}	ν_{12}
G_{12}	G_{13}
G_{13}	G_{23}
G_{23}	G_{12}

Once the materials were defined for the FEA models, meshes of 20-node, reduced integration, brick elements were generated for the tubes tested, beginning with the non-reinforced specimens. The meshes took into account the measured dimensions and steel properties of every specimen. Figure 5 displays the mesh for the non-reinforced tube with external defect. There were 2 elements across the radial direction, both for the steel tubes and the repair materials.

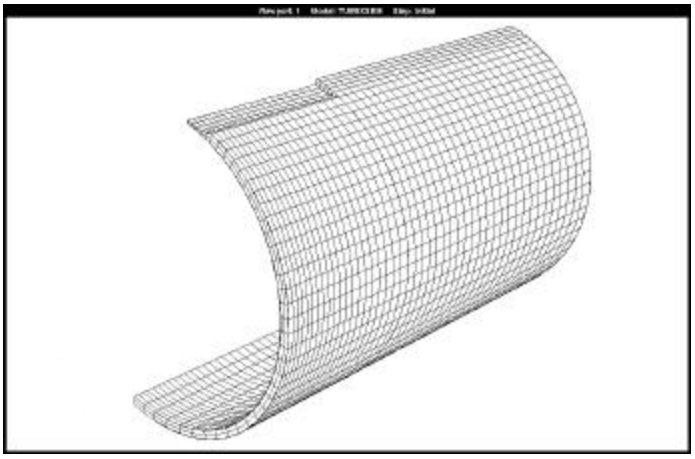

Figure 5 – Finite element mesh of the non-reinforced tube with external defect, taking advantage of the double symmetry.

The comparison between the strains obtained from the numerical analysis and the experimental values for this case is shown in figure 6. The agreement was quite good, even if it is considered that FEA did not model the plastic necking at the final stage of the loading process. The circumferential strain at the external surface of the center of the defect is identified as CC, and the longitudinal strain at the same position is CL.

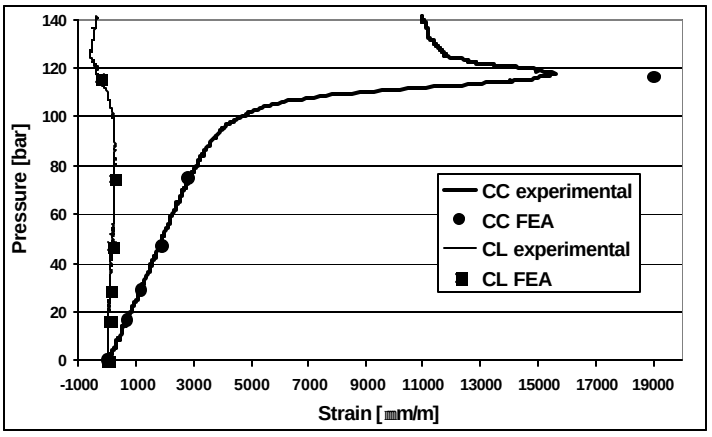

Figure 6 – Comparison between experimental and FEA results for the non-reinforced tube with external defect.

This result encouraged the use of FEA models to describe the behavior of the reinforced tubes. All the repair systems gave similar results, that will be described here by using the results related to the repair system C. The analysis focused on the second pressure cycle, that simulated the hydrotest condition of a new pipeline. The first pressure cycle to 90 percent of the design pressure had the purpose of accommodating the composite material over the metallic tube, but caused some plastic flow in the latter, as mentioned before. The stress-strain curve input for the steel was modified accordingly. The results related to the specimen with internal defect are shown in figure 7.

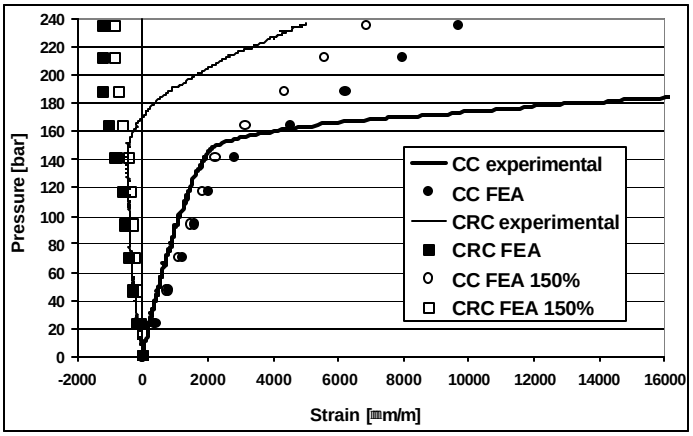

Figure 7 - Comparison between experimental and FEA results for the C repaired tube with internal defect.

As figure 7 shows, at the elastic regime the outer surface of the composite reinforcement actually went into compression, due to the hinge effect of the defect in the metallic tube underneath. The composite sleeve started to effectively reinforce the metallic tube once it began to yield.

The filled symbols in the graph are the FEA results considering the repair properties as shown in table 1. It is apparent that the continuously wrapped fibers developed more circumferential stiffness than the flat tensile test specimens indicated. This behaviour occurred for all the repair systems evaluated. The proposed hypothesis was tried by increasing the longitudinal modulus of the repair laminate, E_1 (or E_2 in the FEA reference system), by 50 percent. The results are shown as empty symbols in figure 7. The circumferential strain in the composite and in the metallic tube as indicated by FEA came closer to the experimental values, the agreement being better for the composite.

Further, the experimental results showed a well-defined bend once the reduced wall thickness in the metallic tube started to yield. The FEA results also displayed a bend, but much less pronounced. The FEA model assumed material continuity between metal and composite, where in fact complex interface behaviour took place. The simple models proposed so far did not consider the interface.

As the adhesive at the interface displays a pronounced non-linear behaviour for in-plane shear loads, a second hypothesis was tried. The continuity between the composite sleeve and the metallic tube was supposed to exist only along the radial direction, with no constraints along the circumferential and axial directions. The comparison between the FEA run incorporating both hypotheses and the experimental results is shown in figure 8. The bends at steel yield point indicated by FEA went closer to the bends observed experimentally.

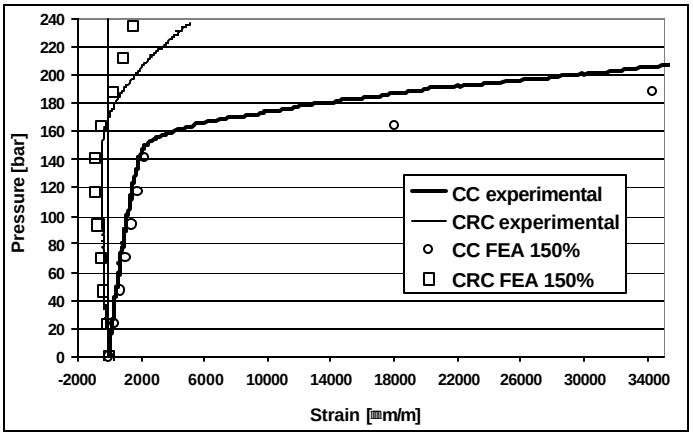

Figure 8 - Comparison between experimental and FEA results for the C repaired tube with internal defect, incorporantig two hypotheses.

Figure 9 shows the experimental results for the specimen with external defect, reinforced with the composite repair system C, for the second pressure test. In this case the reinforcement started to work from the beginning of pressure application, being more effective as the steel tube started to yield. The FEA model is further complicated by the presence of resin to fill the defect. The FEA studies of this case are still underway.

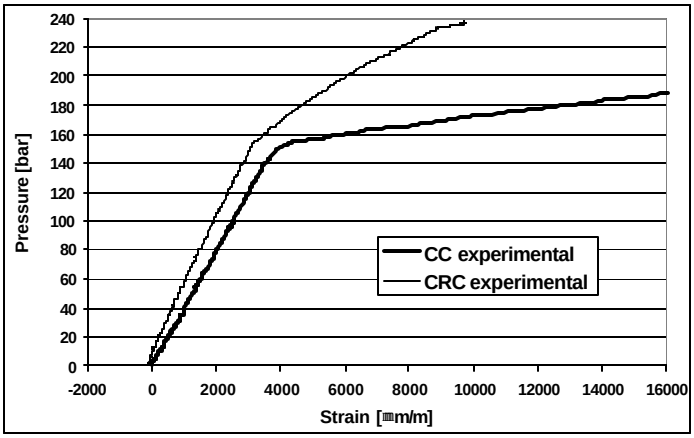

Figure 9 - Experimental results for the C repaired tube with external defect.

CONCLUSIONS

The results indicated that, up to the start of yielding of the pipe defect region, practically only the elastic pipe stresses equilibrated the pressure loading, due to the steel high Young modulus. After yielding, the composite material started working effectively, carrying an important part of the pressure loading increments

Test results showed that three repair systems allowed the pipes to reach the original design pressure. These repairs withstood pressures above those that ruptured similar specimens that were not repaired. However, only one of the repair systems was approved in all strength verification tests for both internal and external defects. This system operated during a minimum of four hours under a hydrostatic pressure test (to the SMYS) and was also able to withstand ten pressure cycles of zero-to-design pressure without showing any visual damage.

The FEA modelling of the tubes tested indicated that further studies are necessary to better describe the stiffness of the repair systems and the behaviour of the interface between composite sleeve and the metallic tube.

ACKNOWLEDGMENTS

The authors would like to acknowledge the support to this research from the Brazilian Ministry of Science and Technology, through the 1999 round of the CTPETRO fund.

REFERENCES

1 – ASME. ”Pipeline Transportation Systems for Liquid Hydrocarbons and Other Liquids, ASME Code for Pressure Piping, B31.4”, The American Society of Mechanical Engineers, New York, 1998.

2 – Benjamin, A.C., Vieira, R.D., Freire J.L.F. e Castro, J.T.P., “Modified Equation for the Assessment of Long Corrosion Defects”. 20th International Conference on Offshore Mechanics and Arctic Engineering, Rio de Janeiro, 2001.

3 - ASME. "Manual for Determining the Remaining Strength of Corroded Pipelines – A Supplement to ASME B31 Code for Pressure Piping, B31.G", The American Society of Mechanical Engineers, New York, 1991.

4 - DNV, "Corroded Pipelines – Recommended Practice RP-F101", Det Norske Veritas, Oslo, 1999.

5 – Varadan, T.K. e Baskhar, K., “Bending of Laminated Orthotropic Cylindrical Shells – An Elasticity Approach”, Composite Structures, 17, 141-156, 1991.

6 – Hibbit, Karlsson and Sorensen. Abaqus Version 6.2 Users Manual, Pawtucket, 2000.

7 – Tsai, S.W. Theory of Composite Design, Think Composites, Dayton, 1992.